

Spin-Coupled Model of the Bonding in First-Row Transition Metal Methylene Monocations

François Ogliaro,[†] Stephen D. Loades,[‡] and David L. Cooper*

Department of Chemistry, University of Liverpool, P.O. Box 147, Liverpool, U.K. L69 7ZD

Peter B. Karadakov

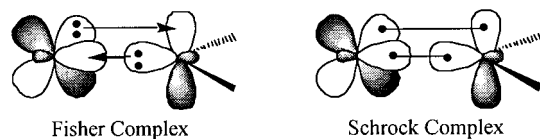
Department of Chemistry, University of Surrey, Guildford, Surrey, U.K. GU2 7XH

Received: December 17, 1999; In Final Form: May 19, 2000

The ab initio spin-coupled model, which is one of the most useful formulations of modern valence bond theory, has been used to study the general characteristics of, and the variations in, the chemical bonding in MCH_2^+ ($M = Sc-Co$) systems. The covalent metal–methylene interaction, characteristic of Schrock complexes, exhibits simultaneously a metal to ligand σ electron donation and a ligand to metal π electron donation. The degree of σ donation decreases and that of π donation increases monotonically from $ScCH_2^+$ to $CoCH_2^+$ in parallel with the decreasing dipole moment of the system and the increasing electronegativity of the M^+ center. The metal–methylene interactions are found to be well described by a balance between two resonant Lewis structures: a dominant doubly bonded closed-shell $^+M=CH_2$ form and a much less important diradical-like, singly bonded form, $^+M\cdot-CH_2$. The importance of this last, which accounts for the triplet character in the π (and σ) interaction(s), grows with the number of unpaired nonbonding electrons on the metal. Such trends may be easily understood in terms of the preservation of intraatomic exchange energy and are consistent with a general decrease in the intrinsic bond strength from $ScCH_2^+$ to $MnCH_2^+$, and vice versa from $MnCH_2^+$ to $CoCH_2^+$. In addition, the sequential filling of nonbonding orbitals across the series is found to originate from a compromise between the minimization of repulsive electrostatic interactions between them and with bonding pairs, and the maximization of the intraatomic exchange energy.

1. Introduction

Transition metal carbenes have been implicated as reactive species and as intermediates in a wide range of important heterogeneous and homogeneous catalytic reactions.¹ More than thirty-five years since the first synthesis of such a system, namely $[(CO)_5WCM_e(OMe)]$ by Fisher and Maasbol,² it is commonplace to distinguish between carbene and alkylidene complexes. Each class of compounds exhibits specific reactivity as a direct manifestation of the specificity of the bonding interaction, being predominantly covalent or dative (see below). Actual metal carbene complexes of Fisher's type present a carbene ligand that is electrophilic, whereas the ligand in metal alkylidene complexes of Schrock's type is nucleophilic. Both types of complex have been intensively studied by computational means.^{3–5}



In this broad family of compounds, it is probably the metal methylene monocations that have the richer experimental history over the last two decades,^{6,7} not least because they play an important role in various reactions such as oligomerizations⁸

[†] Present address: Department of Organic Chemistry and The Lise Meitner-Minerva Center for Computational Quantum Chemistry, Hebrew University, 91904 Jerusalem, Israel.

[‡] Present address: Uniquema, P.O. Box 2, 2800 AA Gouda, The Netherlands.

and because they are perhaps the simplest and smallest carbene complexes imaginable. In the meantime, naked complexes have been the subject of an incredible number of high-level computational surveys,^{5,9–12} in part because of the need for new developments in quantum chemistry to be tested on “sensitive” systems, such as transition metal complexes. Carter and Goddard established that approaches of Hartree–Fock quality fail to describe properly the weak π bond of MCH_2^+ complexes.^{5c}

The purpose of the present work is to use modern valence bond (VB) theory, in its spin-coupled (SC) form, to understand the nature of the metal–ligand binding in these systems. In addition, we want to assess the ability of this method to provide a clear picture of the main chemical features of transition metal complexes. Whereas the SC approach has already proved reliable for a wide range of organic and inorganic systems not containing elements with d orbitals, there have been few clear indications as to how it will perform for transition metal species. Indeed, relatively few ab initio VB studies, such as those in refs 5 and 13–21 have focused on transition metal complexes, with the majority of these dealing with the simplest singly bonded metal–hydrogen^{13,14,18–20} or metal–methyl¹⁵ systems. In our recent work on metal–methylene monoactions,^{16,17} we concentrated on the relative merits of the symmetry-separated $\sigma + \pi$ and symmetry-equivalent Ω bond models of the formal double bond. Our main objective in the present final part is to explain the general tendencies of energy-related and wave function-related characteristics of the chemical bonding across the MCH_2^+ ($M = Sc-Co$) series.

We identify common features of the metal–methylene interaction, using familiar concepts such as electron donation,

hybridization of the metal center, covalent vs ionic character, and so on. Key parameters, such as the number of unpaired electrons, the degree of (partial) triplet character in the bonds, and the electronegativity of the M^+ center, are employed to rationalize variations in the σ and π interactions. The bonding is also analyzed in terms of resonance between simple Lewis structures and we investigate the nature of the difference between the N -electron SC and the corresponding “ N electrons in N orbitals” CASSCF wave functions.²² Variations in SC charge distributions and dipole moments are quantified and explained, and these are compared with values obtained from higher-level CASPT2 calculations.²³ We also elucidate trends in this series with the help of intrinsic binding energies. Intrinsic binding energies are preferred here to standard binding energies because of the way the former can be used in a straightforward manner to furnish some indirect evidence for the pertinence of the SC description of the bonding. Finally, we examine and compare the sequential filling of nonbonding metal orbitals across the $ScCH_2^+ - CoCH_2^+$ series with the analogous order in the diatomic MH^+ systems. Simple and useful qualitative rules emerge for predicting the nature of the ground states of inorganic complexes of the first row, without further calculations.

2. The Spin-Coupled Model

The ab initio spin-coupled wave functions used in the present work take the form²⁴

$$\Psi_{sc} = \mathcal{A} \left[\left(\prod_{i=1}^n \psi_i \alpha \psi_i \beta \right) \left(\prod_{\mu=1}^N \phi_{\mu} \right) \Theta_{SM}^N \right] \quad (1)$$

Functions $\{\phi_{\mu}\}$ are singly occupied nonorthogonal SC orbitals which accommodate the N active electrons. The total wave function Ψ_{sc} is not invariant to arbitrary unitary transformations of these active orbitals, which are thus a unique outcome of the variational procedure. The total spin function for the N active electrons Θ_{SM}^N , labeled according to the eigenvalues of \hat{S}^2 and \hat{S}_z , is expanded in the full spin space²⁵ of f_S^N linearly independent modes of spin coupling:

$$\Theta_{SM}^N = \sum_{k=1}^{f_S^N} c_{Sk} \Theta_{SM,k}^N \quad (2)$$

A fully variational SC calculation consists of the simultaneous optimization of all the spin and orbital degrees of freedom, namely the n inactive orbitals ψ_i , the N active orbitals ϕ_{μ} , and the f_S^N spin-coupling coefficients c_{Sk} . It is important to mention that, unlike classical VB theory, the SC method does not presuppose the form or degree of localization of the orbitals. Furthermore, there are no constraints on the overlaps among the ϕ_{μ} or on the corresponding mode of spin coupling. A particularly simple way of analyzing the active space spin function Θ_{SM}^N is to evaluate spin correlation matrix elements $\langle \hat{s}(\phi_{\mu}) \cdot \hat{s}(\phi_{\nu}) \rangle$, in which $\hat{s}(\phi_{\mu})$ is the one-electron spin operator associated with the electron occupying orbital ϕ_{μ} . Limiting cases are $-3/4$ and $+1/4$ for pure singlet and pure triplet coupling, respectively, and zero for strictly uncoupled electron spins.

In general, a one-configuration N -electron SC wave function is very similar to the corresponding many-configuration “ N electrons in N orbitals” CASSCF function, but it is obviously much more compact and thus easier to interpret. Various strategies may be used to improve the SC model, usually involving excitations into virtual orbitals. In particular, non-

orthogonal configuration interaction calculations starting from a SC or multiconfiguration SC (MCSC) reference function lead to accurate description of ground and excited states.^{24a}

3. Details of the Calculations

The metal–carbon distances were taken from modified coupled-pair formalism (MCPF) ground-state geometry optimizations¹¹ performed in C_{2v} symmetry: in bohr, Sc–C = 3.729, Ti–C = 3.646, V–C = 3.502, Cr–C = 3.407, Mn–C = 3.471, Fe–C = 3.434 and Co–C = 3.386. We adopted C_{2v} symmetry for all the complexes, with z along the C_2 axis and all atoms in the plane $x = 0$. For the sake of simplicity and consistency in the discussion, the CH bond lengths are fixed at 2.078 bohr and the HCH bond angles at 125° . We checked that this approximation for the geometries does not have any significant consequence on our results. Naturally, we examined the same ground states as given in ref 11, namely 1A_1 for $ScCH_2^+$, 2A_1 for $TiCH_2^+$, 3B_2 for VCH_2^+ , 4B_1 for $CrCH_2^+$, 5B_1 for $MnCH_2^+$, 4B_1 for $FeCH_2^+$, and 3A_2 for $CoCH_2^+$. According to the B3LYP calculations reported by Ricca and Bauschlicher,¹⁰ the actual ground state of VCH_2^+ may be 3B_1 instead of 3B_2 , but the computed energy separation between the two states is very small (~ 0.5 kcal/mol) and this reordering originates from zero-point corrections. For consistency with the other systems, we consider here only the 3B_2 state; this choice does not affect in any way the validity of the discussion in section 4D, since in both states, 3B_1 and 3B_2 , one d_δ and one d_π orbital is singly occupied. The B3LYP calculations of ref 10 also suggest that the $ScCH_2^+$ and $TiCH_2^+$ complexes are likely to opt in their ground states for C_s , rather than for C_{2v} symmetry, the symmetry lowering arising from a rotation of the CH_2 group to allow a stabilizing interaction between one of the CH bonds and an empty d orbital on the metal atom. However, the predicted effect on the energy is small, < 2 kcal/mol,¹⁰ so that it is reasonable to adhere to C_{2v} symmetry in the present study.

As in our earlier work,¹⁷ we employed a spherical Gaussian basis set, similar to the one used in ref 11. For the lighter atoms, we used the correlation-consistent Dunning valence triple- ζ (cc-pVTZ) set,²⁶ which corresponds to a [4s3p2d1f] contraction of (10s5p2d1f) primitives for C and to a (5s2p1d)/[3s2p1d] basis for H. The transition metal atoms were described using the (14s9p5d)/[8s4p3d] basis due to Wachters,²⁷ supplemented by the (3f)/[2f] set of polarization functions developed by Bauschlicher et al.,²⁸ thus leading to a final transition metal basis set of the form (14s9p5d3f)/[8s4p3d2f].

The N -electron SC and “ N in N ” CASSCF calculations were carried out with an active space based on the σ and π metal–carbon bonding pairs (i.e., two a_1 orbitals and two b_1 orbitals), augmented with orbitals for any nonbonding electrons on the metal atom. From $TiCH_2^+$ to $MnCH_2^+$ the nonbonding electrons are accommodated by a_1 (l_1), b_2 (l_2), a_2 (l_3), and a_1 (l_4) metal-based orbitals, respectively. The l_1 orbital becomes doubly occupied for $FeCH_2^+$, while in $CoCH_2^+$ the extra electron occupies the l_2 orbital, which makes it necessary to add one a_1 and one b_2 molecular orbital in order to perform an “ N in N ” CASSCF calculation. The optimized forms of the nonbonding orbitals are found to be as follows: l_1 is a $d_\delta = d_{x^2-y^2}$ atomic function on the metal, l_2 is $d_\pi = d_{yz}$, l_3 is $d_\delta = d_{xy}$, and l_4 is a hybrid orbital on the metal, of the form $s + \lambda d_\sigma = s + \lambda d_{2z^2-x^2-y^2}$, “pointing” away from the carbon atom.

We have shown previously^{16,17} that the description of the metal–methylene interaction and of the nonbonding orbitals is little changed when using instead a full-valence active space (i.e., treating as active also the orbitals associated with the CH bonds). In our previous work, we also compared the symmetry

separated ($\sigma + \pi$) and bent bond (Ω) models of the formal double bond in the MCH_2^+ systems, and concluded that the former offers the more appropriate description of the metal–methylene interaction.^{16,17}

All calculations were performed with the MOLPRO suite of programs,²⁹ which now incorporates an efficient modern VB module known as CASVB^{30–33} The SC wave functions were obtained through full simultaneous optimization of the core and valence subspaces. We also report here some *post*-CASSCF calculations which take account of dynamical electron correlation effects; these are based on the perturbation technique known as the CASPT2 formalism, in which the CASSCF wave function provides the reference for a second-order Rayleigh–Schrödinger perturbation theory construction.²³

4. Results and Discussion

A. Bonding Characteristics. The four SC orbitals which describe the metal–methylene bonding in MCH_2^+ ($\text{M} = \text{Sc–Co}$) complexes are displayed in Figure 1. Visual inspection of the form of the orbitals reinforces our conviction¹⁷ in a standard description of the metal–ligand bond at the SC level of theory, making it particularly straightforward to identify general characteristics and trends.

For each system, the bonding pair describing the axial interaction consists of orbitals σ_C and σ_M , the first of which is an sp^x -like hybrid, almost exclusively centered on the carbon atom. Its partner, σ_M , is based on an $s + \lambda d_\sigma$ hybrid centered on the metal, and is deformed toward the methylene fragment. This delocalization of σ_M may be interpreted as an indication of metal to ligand ($\text{M} \rightarrow \text{L}$) electron donation. On the other hand, π_M is an almost pure metal d_π orbital and π_C , which is based principally on a $\text{C}(2\text{p}_\pi)$ function, is significantly deformed toward the metal atom. This nonnegligible contribution of d_π character in the π_C orbital indicates ligand to metal ($\text{M} \leftarrow \text{L}$) electron donation. For each MCH_2^+ complex, the metal center is therefore found systematically to be a σ donor and a π acceptor with respect to the CH_2 group. The M^+ centers becomes increasingly electronegative across the series from Sc^+ to Co^+ , as do their neutral parents.³⁴ Accordingly, the two SC orbitals associated with the metal center, σ_M and π_M , contract on moving from ScCH_2^+ to CoCH_2^+ (see Figure 1).

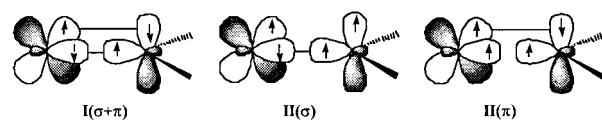
Carter and Goddard^{5a} studied CrCH_2^+ and RuCH_2^+ using the GVB approach, which involves additional constraints, such as strong orthogonality. Nonetheless, the resulting GVB orbitals were fairly similar to those described here. A notable difference concerns σ_M which, in their study, was almost a pure (94.1%) metallic d_{z^2} atomic orbital.

Analysis of the orbital overlaps and spin correlation matrix elements (see Figure 2) shows the σ interaction to be systematically much stronger than the π interaction. The overlap $S_\sigma = \langle \sigma_C | \sigma_M \rangle$, which varies between 0.77 and 0.80, is approximately twice the value of $S_\pi = \langle \pi_C | \pi_M \rangle$ which varies between 0.30 and 0.42. Such values of S_σ are typical of those found for σ bonds in the wide range of systems studied with the SC approach (e.g., 0.81 in FeH , 0.79 in SF_6 , 0.82 in SiH_5^- , 0.81 in CH_2). By contrast, those of S_π are somewhat smaller than we have typically found for π bonds (e.g., 0.62 in C_2H_2 , 0.53 in C_6H_6). Similarly, $\langle \hat{s}(\sigma_C) \cdot \hat{s}(\sigma_M) \rangle$ never exceeds -0.61 , so that there is never more than 14% triplet character in the σ interaction, whereas $\langle \hat{s}(\pi_C) \cdot \hat{s}(\pi_M) \rangle$ can reach -0.42 , which corresponds to 33% triplet character in the π interaction. The relative weakness of the π bond was discussed by Alvarado-Swaigood and Harrison,¹² among others.

We argued previously¹⁷ that the degree of triplet character in the π bond is the result of a competition between the

maximization of intraatomic exchange energy and the preservation of a strong metal–ligand interaction. As shown in Figure 2b, the spin correlation matrix elements $\langle \hat{s}(\pi_C) \cdot \hat{s}(\pi_M) \rangle$ increase with the number of unpaired electrons on the metal, logically reaching a maximum at Mn. The values of $\langle \hat{s}(\sigma_C) \cdot \hat{s}(\sigma_M) \rangle$ show similar behavior, but it is clear that the σ bonding is much less sensitive to the presence of unpaired electrons than is the π interaction. This is not surprising, given that the singlet-coupled σ interaction is much stronger than its π analogue and that orbital σ_M is based on a mixture of 4s and 3d atomic orbitals whereas π_M is essential pure d: in transition metals, the d–d exchange energy is much larger than the s–d exchange energy.³⁵ From Figure 2a, we see that the orbital overlaps are somewhat less sensitive to the number of unpaired electrons than are the spin correlation matrix elements but do show the expected trends: they are reduced both by the orbital contraction upon an increase of the electronegativity of M^+ and by the triplet character in the bond due to the presence of unpaired electrons. These two effects act in cooperation from ScCH_2^+ to MnCH_2^+ leading to decreasing values of S_π and S_σ . From MnCH_2^+ to CoCH_2^+ they act in opposition; the triplet character in the bond prevails over the electronegativity effect, and so we observe in Figure 2a a slight increase of S_π and S_σ .

The three VB-like structures which contribute to the metal–methylene bonding may be represented as



The dominant species $\text{I}(\sigma + \pi)$ is associated with the perfect pairing scheme and corresponds to the classical closed-shell, covalent, doubly bonded description of the metal–methylene interaction. The perfect pairing mode of spin coupling (expressed in the Kotani or Serber bases²⁵) accounts for 98.2, 88.8, 80.0, 68.9, 59.7, 65.8 and 70.2%, respectively, of the total spin function Θ_{SM}^N for the N active electrons in the MCH_2^+ ($\text{M} = \text{Sc–Co}$) complexes; the weight of $\text{I}(\sigma + \pi)$ decreases from ScCH_2^+ to MnCH_2^+ , and increases again afterward. Analysis of the active space spin function also shows that modes corresponding to triplet character in the σ bond are much less important than are those relating to triplet character in the π interaction.³⁶ The minority form $\text{II}(\sigma)$ corresponds to a singlet pairing of the σ electrons and a triplet pairing of π electrons. It is an open-shell, diradical-like singly bonded structure. Finally, there is only a very small contribution from $\text{III}(\pi)$, with triplet pairing of the σ electrons and a singlet-coupled π pair.

Another way of assessing the relative importance of $\text{I}(\sigma + \pi)$, $\text{II}(\sigma)$ and $\text{III}(\pi)$ is to construct an orthogonal natural orbital representation of the SC wave functions, because the three structures correspond to $(\sigma)^2(\pi)^2$, $(\sigma)^2(\pi)^1(\pi^*)^1$ and $(\sigma)^1(\sigma^*)^1(\pi)^2$ configurations, respectively. The occupation of the lowest energy natural orbitals are 1.9755, 1.9735, 1.9708, 1.9529, 1.9294, 1.9450 and 1.9432, respectively, for the σ interaction and 1.7144, 1.6129, 1.5549, 1.3813, 1.4141 and 1.4521, respectively, for the π interaction across the $\text{ScCH}_2^+ \text{–CoCH}_2^+$ series. The trends indicated by these occupation numbers are much the same at the SC, CASSCF, and CASPT2 level of theory.

In terms of Lewis analysis, only two structures are required to account for the metal–methylene interaction:



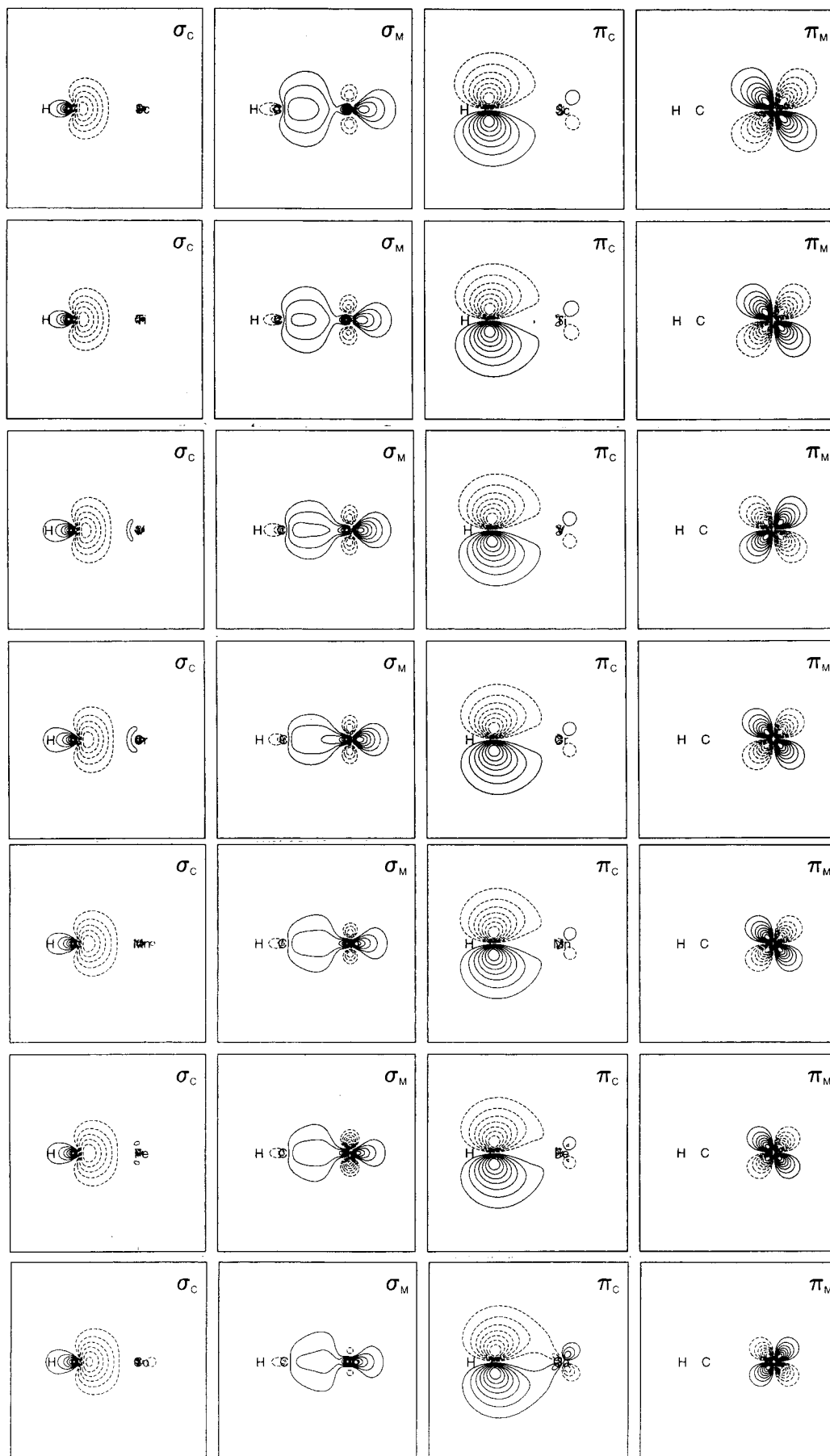


Figure 1. Four SC orbitals involved in the metal–methylene bonding in MCH_2^+ complexes ($M = Sc-Co$, from top to bottom).

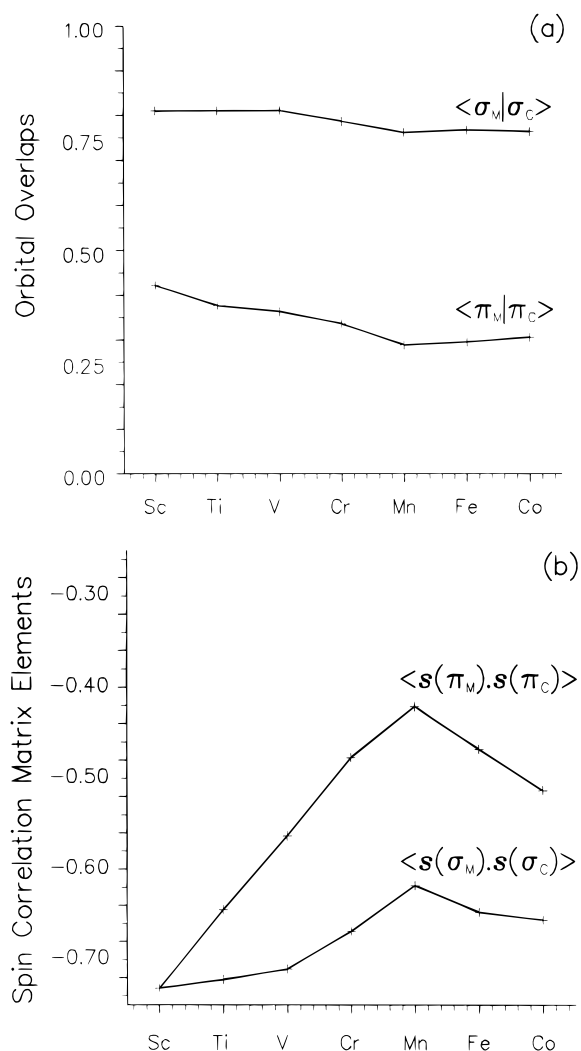


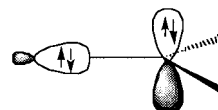
Figure 2. Orbital overlaps and spin correlation matrix elements in the MCH_2^+ series.

since $\mathbf{II}(\sigma)$ and $\mathbf{II}(\pi)$ may be assigned the same Lewis representation. The importance of \mathbf{II} increases from $ScCH_2^+$ to $MnCH_2^+$ and decreases afterward. Of course, one could replace the lines representing purely covalent bonding by arrows, so as to emphasize the dative nature of the interactions.

A purely electrostatic metal–methylene interaction, in a Fisher complex, could be based solely on a d^{n+1} configuration, so that one crude way of estimating the covalent character (deemed to arise from s^1d^n) is to perform a Mulliken population analysis. At the SC level, the d populations are 1.34, 2.35, 3.39, 4.47, 5.08, 6.12 and 7.11, respectively, suggesting covalent character of 66, 65, 61, 53, 92, 88 and 89%, respectively, for the MCH_2^+ ($M = Sc-Co$) complexes. Taking into account also the form of the SC orbitals, this series therefore appears undoubtedly to be of Schrock's type. It should be mentioned that our SC and "N in N" CASSCF wave functions are biased in favor of electronic states with low d occupation whereas the opposite is true¹⁰ for the B3LYP formalism. This can easily be seen by computing the $s^1d^n-d^{n+1}$ energy separations for, e.g., Sc^+ : the SC and CASSCF values are too large, whereas the B3LYP values are too small.

B. Difference between SC and CASSCF Energies. The single-configuration SC wave functions capture between 83 and 90% of the total CASSCF ('nondynamical') correlation energy in the ($M = Sc-Mn$) series.¹⁷ We find that the difference between the two wave functions is concentrated in so-called

doubly ionic configurations, i.e., in those which feature two doubly occupied SC orbitals: MCSC wave functions consisting of the SC configuration plus all doubly ionic configurations recover more than 99% of the CASSCF correlation energy. For each system, a closer examination of these MCSC wave functions reveals that it is just one doubly ionic structure that dominates the difference from the SC energy. For each complex, this additional structure is based on the same $(\sigma_M)^2(\pi_C)^2$ configuration and may be represented graphically as



This particular configuration is not associated with charge transfer, because C and M still have two electrons each. As a consequence, SC and CASSCF calculations should provide similar dipole moments (see below) and, more generally, similar chemical descriptions. A two-configuration SC wave function based on the SC configuration and this particular doubly ionic configuration recovers between 91 and 97% of the CASSCF correlation energy.

C. Dipole Moments and Intrinsic Binding Energies. Dipole moments (μ) and net Mulliken charges (q) computed at the SC, CASSCF and CASPT2 levels are recorded in Table 1. As anticipated, the SC and CASSCF values are fairly similar. The changes on inclusion of dynamical correlation via the CASPT2 formalism are also rather modest.

Each metal–methylene bond is found to be polarized toward the methylene group. The magnitude of the charge separation and of the dipole moment decreases from $ScCH_2^+$ to $CoCH_2^+$. A close inspection of the SC orbitals provides additional insights: on moving from $ScCH_2^+$ to $CoCH_2^+$, the delocalization of σ_M toward the methylene group tends to be reduced while σ_C remains essentially unchanged. These observations are consistent with a reduction of the σ donor capacity of M^+ as its electronegativity increases. At the same time, π_C is found to acquire slightly more metal character: this corresponds to an accentuation of the π acceptor character of M^+ . Naturally, the concurrent decrease across the series of the σ donor capacity of M^+ with respect to the CH_2 group and the reinforcement of its π acceptor capacity results in a decrease in the polarity of the metal–methylene interaction.

General trends in the binding energies across the MCH_2^+ series have been discussed extensively. Revisiting a preliminary experimental study due to Armentrout et al.,⁷ Bauschlicher et al.¹¹ established the existence of a quasi-linear relationship between the dissociation energies and the metal cation *promotion-plus-exchange* energies, as defined and computed by Carter and Goddard.³⁵

An attractive way of examining the strength in situ of the M^+ interaction with CH_2 is to use intrinsic binding energies, defined by Ziegler and co-workers³⁷ as "the difference of energy between the molecule and its subsystems taken in their molecular electronic configurations and considered at their molecular equilibrium geometries." Figure 3 shows intrinsic "experimental" binding energies computed with respect to the s^1d^n dissociation limit.³⁸ Except for a small discontinuity at chromium, the general trend is for the intrinsic bond strengths to decrease from $ScCH_2^+$ to $MnCH_2^+$ and then to increase again beyond this point. This observation is, of course, consistent with our earlier remarks about the increase of the number of unpaired electrons on the transition metal which confers a higher weight to the singly bonded structures \mathbf{II} . Also shown in Figure 3 are

TABLE 1: Dipole Moments^a (μ , in Debye) and Net Mulliken Charges (q)

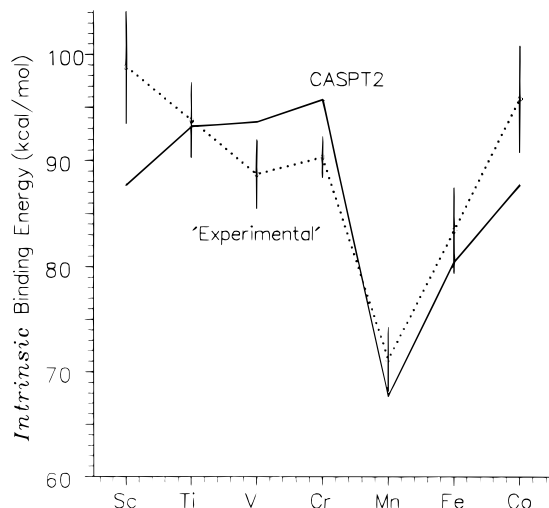
	ScCH ₂ ⁺	TiCH ₂ ⁺	VCH ₂ ⁺	CrCH ₂ ⁺	MnCH ₂ ⁺	FeCH ₂ ⁺	CoCH ₂ ⁺
μ (CASPT2)	5.67	4.75	4.34	3.72	3.02	2.74	2.06
μ (CASSCF)	5.69	4.80	4.32	3.69	3.09	2.78	2.05
μ (SC)	5.72	4.96	4.52	3.93	3.33	3.29	2.89
q_M (CASPT2)	1.47	1.42	1.43	1.38	1.37	1.36	1.31
q_C (CASPT2)	-0.83	-0.80	-0.78	-0.73	-0.75	-0.74	-0.67
q_M (CASSCF)	1.47	1.43	1.41	1.36	1.37	1.36	1.30
q_C (CASSCF)	-0.82	-0.79	-0.75	-0.70	-0.75	-0.74	-0.66
q_M (SC)	1.49	1.46	1.45	1.40	1.40	1.43	1.40
q_C (SC)	-0.85	-0.83	-0.79	-0.73	-0.78	-0.80	-0.75

^a The origin is at the center of mass.

TABLE 2: Ground States (GS) and Electronic Configurations for the MH⁺ and Series

nb ^a	MCH ₂ ⁺	GS ^b	configuration ^b	MH ⁺	GS ^c	configuration ^c
0	ScCH ₂ ⁺	¹ A ₁	(σ) ² (π) ²	ScH ⁺	² Δ	(σ) ² (d _δ)
1	TiCH ₂ ⁺	² A ₁	(σ) ² (π) ² (d _δ)	TiH ⁺	³ Φ	(σ) ² (d _δ) ¹ (d _π) ¹
2	VCH ₂ ⁺	³ B ₂	(σ) ² (π) ² (d _δ) ¹ (d _π) ¹	VH ⁺	⁴ Δ	(σ) ² (d _δ) ¹ (d _π) ¹ (d _π) ¹
3	CrCH ₂ ⁺	⁴ B ₁	(σ) ² (π) ² (d _δ) ¹ (d _π) ¹ (d _δ) ¹	CrH ⁺	⁵ Σ ⁺	(σ) ² (d _δ) ¹ (d _π) ¹ (d _π) ¹ (d _δ) ¹
4	MnCH ₂ ⁺	⁵ B ₁	(σ) ² (π) ² (d _δ) ¹ (d _π) ¹ (d _δ) ¹ (s + λ d _σ) ¹	MnH ⁺	⁶ Σ ⁺	(σ) ² (d _δ) ¹ (d _π) ¹ (d _π) ¹ (d _δ) ¹ (s + λ d _σ) ¹
5	FeCH ₂ ⁺	⁴ B ₁	(σ) ² (π) ² (d _δ) ² (d _π) ¹ (d _δ) ¹ (s + λ d _σ) ¹	FeH ⁺	⁵ Δ	(σ) ² (d _δ) ² (d _π) ¹ (d _π) ¹ (d _δ) ¹ (s + λ d _σ) ¹
6	CoCH ₂ ⁺	³ A ₂	(σ) ² (π) ² (d _δ) ² (d _π) ² (d _δ) ¹ (s + λ d _σ) ¹			

^a Number of unpaired electrons on the metal center. ^b Reference 11. ^c Reference 21.

**Figure 3.** Intrinsic binding energies in the MCH₂⁺ series.

CASPT2 intrinsic binding energies; the corresponding CASSCF and SC results are smaller, because of the neglect of dynamical electron correlation, but they follow the same general pattern as the experimental values.

D. Ground-State Configurations. So far, no full rationalization has been proposed for the successive ordering of molecular states for the MCH₂⁺ (M = Sc–Co) series. On the other hand, a qualitative prediction of the ground state and of low-lying excited states for other transition-metal complexes, based on simple and intuitive arguments, has proved to be rather reliable.²⁰ Almost simultaneously, independent studies due to Loades et al.^{18,19} and to Ohanessian and Goddard²¹ pointed out that the sequence in which the available nonbonding orbitals become occupied across the MH⁺ and MH systems occurs in a consistent manner. We have found that a very similar sequence applies to the complexes considered here: electronic configurations of ground states of MCH₂⁺ and MH⁺ species are compared in Table 2.

The main considerations in determining the occupancy of the nonbonding orbitals l_i appear to be minimization of the electrostatic repulsion between them and with the two bonding pairs σ_C, σ_M and π_C, π_M , and maximization of the number of

unpaired electrons. In this way, a d orbital in the plane perpendicular to the molecular axis is occupied first, because this tends to minimize any interaction with the bonding electrons. Thus, in the MH⁺ diatomics and in the metal–methylene series, the first odd electron is housed in a d_δ orbital. The second nonbonding electron occupies a d_π orbital in preference to the second d_δ orbital. Although this produces a greater electrostatic repulsion with the bonding pairs in comparison with the case in which a further d_δ orbital would be occupied, the d_π orbital is preferentially occupied because filling two orbitals placed in the same plane would produce a more destabilizing effect. In accord with the policy of minimizing repulsive bonding/nonbonding electrostatic interactions, the third additional nonbonding electron of the MH⁺ systems is accommodated in the second d_π orbital, which is orthogonal to all of the previously occupied orbitals. Of course, this d_π component is not available in the MCH₂⁺ series, because it is already involved in the metal–methylene π bond. As a consequence, it is the second d_δ orbital which accommodates the third extra electron for the metal–methylene systems. This is the orbital that is occupied by the fourth nonbonding electron of the MH⁺ systems. Next in the sequence comes an s + λ d_σ hybrid that points away from the ligand. At this stage, all of the available nonbonding orbitals are singly occupied. For FeCH₂⁺, the fifth nonbonding electron is accommodated by one of the d_δ orbitals, which becomes doubly occupied, while in CoCH₂⁺ the second doubly occupied orbital is d_π, following again the same order as seen for TiCH₂⁺ and VCH₂⁺.

Our results clearly indicate that the sequential filling of nonbonding orbitals for the (M = Sc–Co) complexes does not occur in a random manner: nonbonding orbitals are filled in the same order as for the diatomic MH⁺ species, except that one of the d_π orbitals is already involved in bonding. This sequence results from a compromise between minimizing electrostatic repulsions and maximizing the number of unpaired electrons, and thus maximizing the exchange energy.

5. Concluding Remarks

We have found that the spin-coupled description of the metal–methylene interaction is consistent across the whole MCH₂⁺ (M = Sc–Co) series. The bonding is significantly

covalent (arising from s^1d^n configurations) but the M^+ center is simultaneously a σ donor and a π acceptor with respect to the methylene fragment. For these two reasons, all complexes in the series are best described as being of Schrock's type rather than Fischer's type, i.e., as being alkylidene rather than carbene. The continued decrease in the degree of σ donation and the accentuation of the π donation on moving from $ScCH_2^+$ to $CoCH_2^+$, which parallels the increasing electronegativity of the metal center, results in a concomitant decay of the dipole moment.

The metal–methylene interaction may be visualized in terms of just two resonant Lewis structures: a predominant classical closed-shell form **I**, $^+M = CH_2$, together with a minority diradical-like form **II**, $^+M^{\bullet}-\dot{C}H_2$, corresponding to triplet character in the π interaction or, to a much lesser extent, in the σ interaction. The differences between the N -electron SC and corresponding " N in N " CASSCF descriptions are small and consistent: all along the series the difference between these two wave functions consists mostly of the same "ionic" configuration(s). These last do not change the essential description of the bonding.

From $ScCH_2^+$ to $MnCH_2^+$, the increasing number of unpaired electrons accentuates the triplet character in the π (and σ) interaction(s), resulting in an increased weight for the singly bonded structure(s) **II**, and corresponds to a reduction in the intrinsic bond strength. The reverse situation occurs, of course, for the $MnCH_2^+ - CoCH_2^+$ triad.

The sequential filling of nonbonding orbitals in the $MnCH_2^+$ and MH^+ series can easily be understood by considering merely the best way to maximize the exchange energy of unpaired electrons on the metal center and to minimize their electrostatic repulsion with the bonding electrons and with the other electrons of the methylene group. It seems reasonable to suppose that analogous qualitative arguments will work equally well for a wide range of complexes containing first-row transition metal atoms.

Our various results indicate clearly the utility of modern valence bond theory, in its spin-coupled form, for understanding the bonding in complexes that contain transition metal atoms in low oxidation states.

References and Notes

- (1) See, for example: (a) Dötzt, K. H.; Fisher, H.; Hoffman, P.; Kreissl, F. R.; Schubert, U.; Weiss, K. *Transition Metal Carbene Complexes*; Chemie Ed: Deerfield Beach, FL, 1984. (b) Gallop, M. A.; Roper, W. R. *Adv. Organomet. Chem.* **1986**, *25*, 121. (c) Roper, W. R. *Advances in Metal Carbene Chemistry*; Kluwer: New York, 1989.
- (2) Maasbol, A.; Fischer, E. O. *Angew. Chem.* **1964**, *76*, 645; *Angew. Chem., Int. Ed. Engl.* **1964**, *3*, 580.
- (3) For pioneering studies see, for instance: (a) Spangler, D.; Wendoloski, J. J.; Dupuis, M.; Chen, M. M. L.; Schaefer, H. F. *J. Am. Chem. Soc.* **1981**, *103*, 3985. (b) Schoeller, W. W.; Aktekin, N. *J. Chem. Soc., Chem. Com.* **1982**, *20*. (c) Nakatsujii, H.; Ushio, J.; Han, S.; Yonezawa, T. *J. Am. Chem. Soc.* **1983**, *105*, 426. (d) Taylor, T. E.; Hall, M. B. *J. Am. Chem. Soc.* **1984**, *106*, 1576.
- (4) For more recent studies see, for example: (a) Bare, W. D.; Citra, A.; Trindle, C.; Andrews, L. *Inorg. Chem.* **2000**, *39*, 1204. (b) Nguyen, M. T.; Nguyen, T. L.; Le, H. T. *J. Phys. Chem. A* **1999**, *103*, 5758. (c) Su, M.-D.; Chu, S. Y. *Inorg. Chem.* **1999**, *38*, 4819. (d) Vyboishchikov, S. F.; Frenking, G. *Chem. A Eur. J.* **1998**, *4*, 1428. (e) Kemnitz, C. R.; Karney, W. L.; Borden, W. T. *J. Am. Chem. Soc.* **1998**, *120*, 3499. (f) Wang, C. C.; Wang, Y.; Liu, H. J.; Lin, K. J.; Chou, L. K.; Chan, K.-S. *J. Phys. Chem. A* **1997**, *101*, 8887. (g) Jacobsen, H.; Ziegler, T. *Inorg. Chem.* **1996**, *35*, 775.
- (5) For early GVB studies see: (a) Carter, E. A.; Goddard, W. A. *J. Am. Chem. Soc.* **1986**, *108*, 4746. (b) *Ibid.* **1986**, *108*, 2180. (c) *Idem.* *J. Phys. Chem.* **1984**, *88*, 1485.
- (6) (a) Husband, J.; Aguirre, F.; Thompson, C. J.; Laperle, C. M.; Metz, R. B. *J. Phys. Chem. A* **2000**, *104*, 2020. (b) Trost, B. M. *Chem. A Eur. J.* **1998**, *12*, 2405. (c) Chen, Y. M.; Armentrout, P. B. *J. Phys. Chem.* **1995**, *99*, 10775. (d) Haynes, C. L.; Chen, Y. M.; Armentrout, P. B. *J. Phys. Chem.* **1995**, *99*, 9110. (e) Haynes, C. L.; Armentrout, P. B.; Perry, J. K.; Goddard, W. A. *J. Phys. Chem.* **1995**, *99*, 6340. (f) Kemper, P. R.; Bushnell, J.; van Koppen, P. A. M.; Bowers, M. T. *J. Phys. Chem.* **1993**, *97*, 1810. (g) van Koppen, P. A. M.; Kemper, P. R.; Bowers, M. T. *J. Am. Chem. Soc.* **1992**, *114*, 1083.
- (7) Armentrout, P. B.; Sunderlin, L. S.; Fisher, E. R. *Inorg. Chem.* **1989**, *28*, 3845.
- (8) Irikura, K. K.; Beauchamp, J. L. *J. Phys. Chem.* **1991**, *95*, 8344.
- (9) (a) Li, J. H.; Feng, D. C.; Feng, S. Y. *Sci. Chin. Ser. B—Chem.* **1999**, *42*, 83. (b) Li, J. H.; Feng, D. C.; Feng, S. Y. *J. Chin. Universities* **1998**, *19*, 1495. (c) Chen, Q.; Auberry, K. J.; Freiser, B. S. *Int. J. Mass Spectrosc.* **1998**, *175*, 1. (d) Abashkin, Y. G.; Burt, S. K.; Kusso, N. *J. Phys. Chem. A* **1997**, *101*, 8085. (e) Musaev, D. G.; Morokuma, K. *J. Phys. Chem.* **1996**, *100*, 11600. (f) Musaev, G.; Morokuma, K.; Koga, N.; Nguyen, K. A.; Gordon, M. S.; Cundari, T. R. *J. Phys. Chem.* **1993**, *97*, 11435. (g) Heinemann, C.; Hertwig, R. H.; Wesendrup, R.; Koch, W.; Schwarz, H. *J. Am. Chem. Soc.* **1995**, *117*, 495. (h) Blomberg, M. R. A.; Siegbahn, P. E. M.; Svenson, M. *J. Phys. Chem.* **1994**, *98*, 2062. (i) Musaev, D. G.; Koga, N.; Morokuma, K. *J. Phys. Chem.* **1993**, *97*, 4964. (j) Musaev, D. G.; Morokuma, K.; Koga, N. *J. Chem. Phys.* **1993**, *99*, 7859. (k) Bauschlicher, C. W.; Partridge, H.; Scuseria, G. E. *J. Chem. Phys.* **1992**, *97*, 7471. (l) Cundari, T. R.; Gordon, M. S. *J. Phys. Chem.* **1992**, *96*, 631.
- (10) Ricca, A.; Bauschlicher, C. W. *Chem. Phys. Lett.* **1995**, *245*, 150.
- (11) Bauschlicher, C. W.; Partridge, H.; Sheehy, J. A.; Langhoff, S. R.; Rosi, M. *J. Phys. Chem.* **1992**, *96*, 6969.
- (12) Alvarado-Swaisgood, A. E.; Harrison, J. F. *J. Phys. Chem.* **1988**, *92*, 2757.
- (13) (a) Shilling, J. B.; Goddard, W. A.; Beauchamp, J. L. *J. Phys. Chem.* **1987**, *91*, 4470. (b) *Idem.* *J. Am. Chem. Soc.* **1987**, *109*, 5565. (c) *Idem.* *J. Phys. Chem.* **1987**, *91*, 5616. (d) *Idem.* *J. Am. Chem. Soc.* **1987**, *108*, 582.
- (14) Galbraith, J. M.; Shurki, A.; Shaik, S. *J. Phys. Chem. A* **2000**, *104*, 1262.
- (15) (a) Shurki, A.; Hiberty, P. C.; Shaik, S. *J. Am. Chem. Soc.* **1999**, *121*, 9768. (b) Schilling, J. B.; Goddard, W. A.; Beauchamp, J. L. *J. Am. Chem. Soc.* **1987**, *109*, 5573.
- (16) Ogliaro, F.; Cooper, D. L.; Karadakov, P. B. *Int. J. Quantum Chem.* **1999**, *74*, 223.
- (17) Ogliaro, F.; Loades, S. D.; Cooper, D. L.; Karadakov, P. B. *Prog. Theor. Chem. Phys.*, in press.
- (18) Loades, S. D.; Cooper, D. L.; Gerratt, J.; Raimondi, M. *J. Chem. Soc., Chem. Commun.* **1989**, 1604.
- (19) Loades, S. D. Ph.D. Thesis, University of Liverpool, 1992.
- (20) Anslyn, E. A.; Goddard, W. A. *Organometallics* **1989**, *8*, 1550 and references therein.
- (21) Ohanessian, G.; Goddard, W. A. *Acc. Chem. Res.* **1990**, *23*, 386.
- (22) (a) Werner, H.-J.; Knowles, P. J. *J. Chem. Phys.* **1985**, *82*, 5053. (b) Knowles, P. J.; Werner, H.-J. *Chem. Phys. Lett.* **1985**, *115*, 255.
- (23) Werner, H.-J. *Mol. Phys.* **1996**, *89*, 645.
- (24) For reviews see: (a) Cooper, D. L.; Gerratt, J.; Raimondi, M. *Chem. Rev.* **1991**, *91*, 929 and references therein. (b) Gerratt, J.; Cooper, D. L.; Karadakov, P. B.; Raimondi, M. *Chem. Soc. Rev.* **1997**, *26*, 87.
- (25) For an account of the construction of spin bases see, for example: Pauncz, R. *Spin Eigenfunctions*; Plenum Press: New York, 1979.
- (26) Dunning, T. H. *J. Chem. Phys.* **1989**, *90*, 1007.
- (27) Wachters, A. J. H. *J. Chem. Phys.* **1970**, *52*, 1033.
- (28) Bauschlicher, C. W.; Langhoff, S. R.; Barnes, L. A. *J. Chem. Phys.* **1989**, *91*, 2399.
- (29) MOLPRO is a package of ab initio programs written by H.-J. Werner and P. J. Knowles, with contributions from R. D. Amos, A. Berning, D. L. Cooper, M. J. O. Deegan, A. J. Dobbyn, F. Eckert, C. Hampel, T. Leininger, R. Lindh, A. W. Lloyd, W. Meyer, M. E. Mura, A. Nicklass, P. Palmieri, K. Peterson, R. Pitzer, P. Pulay, G. Rauhut, M. Schütz, H. Stoll, A. J. Stone, and T. Thorsteinsson.
- (30) Cooper, D. L.; Thorsteinsson, T.; Gerratt, J. *Adv. Quantum Chem.* **1999**, *32*, 51.
- (31) See for example: Cooper, D. L.; Thorsteinsson, T.; Gerratt, J. *Int. J. Quantum Chem.* **1997**, *65*, 430 and references therein.
- (32) Thorsteinsson, T.; Cooper, D. L. In *Quantum Systems in Chemistry and Physics*; Hernandez-Laguna, A., Mariani, J., McWeeny, R., Wilson, S., Eds.; Kluwer: Dordrecht, 2000; Vol. 1, pp 303–326.
- (33) Thorsteinsson, T.; Cooper, D. L.; Gerratt, J.; Karadakov, P. B.; Raimondi, M. *Theor. Chim. Acta* **1996**, *93*, 343.
- (34) Electronegativity of the neutral metal atom M ($M = Sc-Co$) in the Sanderson scale [Sanderson, R. T. *J. Chem. Educ.* **1988**, *65*, 112] respectively 1.20, 1.32, 1.45, 1.56, 1.60, 1.64, 1.70; in the Allred-Rochow scale [Allred, A. L.; Rochow, E. G. *J. Inorg. Nucl. Chem.* **1958**, *5*, 264] respectively 1.02, 1.09, 1.39, 1.66, 2.20, 2.56.
- (35) Carter, E. A.; Goddard, W. A. *J. Phys. Chem.* **1988**, *92*, 5679.

(36) See Tables 3 and 4 of ref 17.

(37) Ziegler, T.; Tschinke, V.; Ursenbach, C. *J. Am. Chem. Soc.* **1987**, *109*, 4825.

(38) Intrinsic binding energies derived from experimental data for the MCH_2^+ ($M = Sc-Co$) series are 98.8 ± 5.3 , 93.8 ± 3.5 , 88.7 ± 3.2 , 90.3 ± 1.9 , 71.2 ± 3.0 , 83.4 ± 4.0 , and 95.8 ± 5.0 kcal/mol, respectively. Raw experimental energies were taken from Armentrout's experimental work, as converted to 0 K by Bauschlicher et al. and then, if the isolated metal

atom presents a d^{n+1} ground state, the experimental $s^1d^n-d^{n+1}$ energy separation [NIST Atomic Spectra Database (http://physics.nist.gov/cgi-bin/AtData/main_asd)] was subtracted. Based on RCCSD(T) calculations (cc-pVTZ basis) of the energy separation between free CH_2 and the fragment in the complexes, a (fixed) correction of 1.9 kcal/mol was included. The corresponding CASPT2 values of 87.7, 93.2, 93.6, 95.7, 67.7, 80.4, and 87.7 kcal/mol incorporate an approximate 5 kcal/mol correction due to basis set incompleteness and zero-point motion, as discussed in ref 11.